

The preparation and characterization of $\text{TiO}_2/\text{ZrO}_2$ composites doped with PMA/PWA

Thanganathan UMA[†] and Masayuki NOGAMI

Department of Materials Science and Engineering, Nagoya Institute of Technology, Showa, Nagoya 466-8555

A new class of glass composite membranes of various compositions was prepared via a sol-gel technique. The membranes, consisting of (phophotungsticacid/phosphomolybdicacid) PWA/PMA- P_2O_5 - SiO_2 mixed with either ZrO_2 or TiO_2 displayed varying properties depending on their composition and mode of fabrication. The structure and property of the obtained glass ceramic composite membranes were investigated by FTIR, TG/DTA and textural analysis. The results included good mechanical, textural and thermal properties and the materials were deemed to be suitable electrolytes for fuel cell applications.

©2009 The Ceramic Society of Japan. All rights reserved.

Key-words : Glass, Heteropolyacids, FTIR, Thermal, Textural

[Received August 14, 2008; Accepted December 18, 2008]

1. Introduction

While significant advances have been made in recent years with regard to proton conducting membranes, major drawbacks of the current technology include cost and material limitations. The heteropolyacid (HPA) family of membranes is currently the best developed proton conduction membranes that can be operated at both low and high temperatures.^{1,2)} For transport applications, fuel cell companies require more durable, cost-effective membrane technologies that are capable of delivering enhanced products at low temperatures (from room temperature up to 80°C).³⁾⁻⁵⁾ Research is consequently being directed into a wide range of novel organic and inorganic materials with the potential of being promising proton conductors and forming coherent membranes.

The aim of the present investigation was the development of a new class of proton conducting glass membranes for fuel cells. Since increasing or changing the operating properties of fuel cells is not an energy efficient solution, it is preferred to modify the properties of the proton conducting membrane and to enhance its water retention. For that purpose, an incorporation of heteropolyacids into the membrane material has been attempted, where phosphosilicate glass was used to increase the pore size, conductivity and cell performances. Novel glass composite membranes for use in a new class of high-performance fuel cells are being developed. These nano-engineered glass-ceramic proton-conducting membranes are expected to yield high proton conductivities, as well as excellent thermal and chemical stabilities. The work of Nogami et al.⁶⁾⁻⁸⁾ has led to the discovery of a series of functionalized phosphosilicate glass including either zirconium or titanium with interesting proton conducting properties. Our recent work⁹⁾⁻¹¹⁾ has focused on PWA and PMA glass membranes synthesized by a sol-gel process with P_2O_5 - SiO_2 and either ZrO_2 or TiO_2 . Phosphosilicate glasses are well known for their fast-proton conductivity, and attributed to strong hydrogen bonds between water molecules and the P = OH groups of the glass surface. The present investigation concerns the synthesis and characterization — according to our previous work⁹⁾⁻¹¹⁾ —

of a new class of ((phophotungsticacid/phosphomolybdicacid) PWA/PMA- ZrO_2 - P_2O_5 - SiO_2 and PWA/PMA- TiO_2 - P_2O_5 - SiO_2) glass composite membranes.

2. Experimental section

2.1 Preparation of glasses

All used materials was received and prepared according to a procedure that is described in details elsewhere.^{9),10)} The reaction process when going from metal alkoxides to glass was complex due to the reaction conditions and the chemicals used. The process started with the hydrolysis of TEOS (tetraethoxysilane) with a solution of H_2O (as 0.15 N HCl) and $\text{C}_2\text{H}_5\text{OH}$. Di-isopropylphosphate (from Wako Pure Chemical Industries Ltd.) was added dropwise to the above solution under stirring. The phosphorus compound was mixed with the total solution and was stirred for approximately 1 h. PWA and PMA were individually added to the starting solution in appropriate amounts with a 1 h interval. Subsequently, $\text{Ti}(\text{OC}_4\text{H}_9)_4$ and $\text{Zr}(\text{OC}_4\text{H}_9)_4$ were added to the mixture and stirred for 2 h.

The resultant solution was hydrolyzed for a second time by adding H_2O (as 0.15N-HCl aq) and $\text{C}_2\text{H}_5\text{OH}$, after which 1 ml of dimethyl formamide (DMF) was added as a drying condition control agent under magnetic stirring for 30 min. The reaction was allowed to proceed at room temperature for one more hour, after which time a clear homogenous solution was obtained, which formed a gel glass. The gels were dried at room temperature and this was followed by a water- and heat treatment at 150°C and 600°C for 30 h and 2 h, respectively. The thickness of the so-obtained glass composite membranes ranged from 0.5 to 1.5 mm.

2.2 Characterization of glass

The glass materials displayed large pore sizes and surface areas, as determined by analysis of their textural properties. These textural characteristics were obtained from a Quantachrome Instruments-NOVA-1000 nitrogen gas sorption analyzer. Values of specific surface areas, pore diameters and adsorption pore volumes were determined from N_2 - adsorption/desorption isotherms. The pore surface areas were calculated by applying the Barrett-Joyner-Halenda (BJH) method to the desorption

[†] Corresponding author: T. Uma; E-mail: ptuma2002@yahoo.co.in

branches of the isotherms,^{12,13} whereas the specific surface areas were calculated from the BET equation. Prior to the experiments, the samples were degassed at 250°C for 7 h. When a condensed gas is introduced at low vapor pressure, a molecular adsorption layer is first formed on the inner surface of the pores. When the relative pressure P/P_0 of the condensable gas is increased further from zero to unity, pores with increasingly large radii become blocked due to capillary condensation. The simultaneous gas flux through the remaining open pores thus provides a measure of the fraction of pores with pore sizes larger than the pores that are already blocked. Upon desorption the same processes occur in reverse order.

FTIR absorption spectra of the glass composite membranes were recorded with a JASCO FTIR-460 spectrometer (spectral range 4000–600 cm⁻¹, 50 scans, and a resolution of 2 cm⁻¹). All the samples were heated at 60°C under vacuum for 1 h before the measurement. The thermal properties of the glass composite were investigated by TGA and DTA measurements in air. The samples were ramped from room temperature to 800°C at 5°C/min. The reference used for the DTA measurement was $\alpha\text{-Al}_2\text{O}_3$, which was heated at 800°C for 2 h before use. The thermogravimetric analysis of the glass composite membranes was performed using a Thermoplus-2, TG-8120 under a flow of nitrogen.

3. Results and discussion

3.1 Pore study

Figure 1 shows the structural changes due to the presence of ZrO_2 and TiO_2 as determined by the comparison of adsorption-desorption isotherms of PWA/PMA– $\text{ZrO}_2\text{-P}_2\text{O}_5\text{-SiO}_2$ and PWA/PMA– $\text{TiO}_2\text{-P}_2\text{O}_5\text{-SiO}_2$ glass composite membranes. In Figs. 1(a) and (b), the shape of the hysteresis loop indicated changes in the mesopore size and shape. The adsorption-desorption isotherm of PWA/PMA– $\text{ZrO}_2\text{-P}_2\text{O}_5\text{-SiO}_2$ showed a small hysteresis at around $P/P_0 = 0.3$ to 0.4 partial pressure and the adsorption-desorption isotherms of PWA/PMA– $\text{TiO}_2\text{-P}_2\text{O}_5\text{-SiO}_2$ displayed a rather unclear hysteresis loop at around $P/P_0 = 0.4$ to 0.45 partial pressure, signifying that the material was mesoporous.

Hysteresis loops are characteristic for mesoporous materials consisting of spherical particles with a relatively wide pore size distribution and a pore shape that is often described as of ink-bottle type. The main factors that can cause a narrowing of the hysteresis loop include increased pore connectivity and/or a decreased tortuosity. According to the percolation theory,¹⁴⁾ the more highly connected the pore network is, the easier it becomes for vapor-filled pores to form a spanning cluster, and conse-

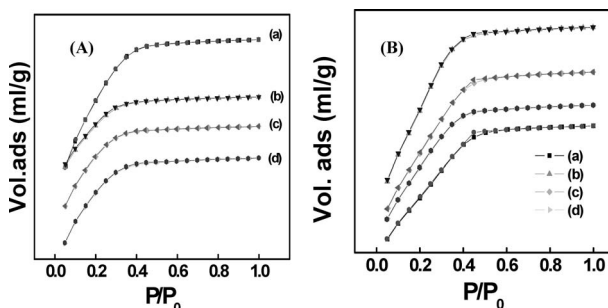


Fig. 1. N_2 adsorption–desorption isotherms of (A) PWA/PMA– $\text{ZrO}_2\text{-P}_2\text{O}_5\text{-SiO}_2$ and (B) PWA/PMA– $\text{TiO}_2\text{-P}_2\text{O}_5\text{-SiO}_2$ glass composite membranes: (a) 1/1–2–5–91 (mol %), (b) 1/1–3–5–90 (mol %), (c) 1/1–4–5–89 (mol %) and (d) 1/1–5–5–88 (mol %).

quently the hysteresis loop becomes narrower. High tortuosity values are normally associated with wide hysteresis loops provided that there is no substantial interference of metastability effects in capillary condensation.¹⁴⁾

The shapes of the hysteresis loops differed greatly with various concentrations of ZrO_2 and TiO_2 . The average pore size generally provides the mechanical strength of a glass composite membrane and for the PWA/PMA– $\text{ZrO}_2\text{-P}_2\text{O}_5\text{-SiO}_2$ (Fig. 2(a)) and PWA/PMA– $\text{TiO}_2\text{-P}_2\text{O}_5\text{-SiO}_2$ (Fig. 2(b)) glass composite membranes, it was 2.15 nm and 2.35 nm, respectively. The pore size was observed to decrease, when increasing the amount of ZrO_2 and TiO_2 . As the pore size decreased, the pores became filled with the water molecules at low humidity, which acted to form the pathways for the proton transfer.¹⁵⁾ The changes in specific surface area and pore volume were due to the polycondensation reaction between the hydroxyl groups of the pore surfaces. The pore volume decreased from 0.27 to 0.19 cm³/g with an increasing concentration of ZrO_2 (Fig. 1(a)) and went from 0.22 to 0.31 cm³/g when increasing the concentration of TiO_2 was raised (Fig. 1(b)). The textural properties were strongly linked to the preparation of the glass and the amount of DMF used in the synthesis. The incorporation of formamide in the sol-gel glass could be responsible for the significant improvement in the protonic conduction for the glass that was heat treated at 600°C. The mechanical stability improvement could also be attributed to the higher porosity of the glass.¹⁶⁾ In this case; a smaller pore size and surface area were observed for the TiO_2 -doped $\text{P}_2\text{O}_5\text{-SiO}_2\text{-PMA}$ glass composite membranes as compared to samples from a previous report.¹¹⁾

3.2 Thermal study

Figures 3(a) and (b) illustrate the TGA thermograms of PWA/PMA– $\text{ZrO}_2\text{-P}_2\text{O}_5\text{-SiO}_2$ and PWA/PMA– $\text{TiO}_2\text{-P}_2\text{O}_5\text{-SiO}_2$, respectively. The thermal decomposition temperature can be taken directly from the TGA curves as the temperature that corresponds to the starting point of an obvious weight loss of the samples. It can be seen in Figs. 3(a) and (b), that the first decomposition temperature occurred at 200 and 150°C, that a second decomposition took place at 350 and 450°C, after which there was a continuous weight loss up to 800°C for all samples. Weight losses of 3.6% and 5% were calculated from the TGA curves. The gradual weight loss of 1.2 and 3.6% within the temperature range of 30 to 450°C was associated with the condensation of OH groups in the glass network structure (Fig. 3(a)). The total weight loss observed was restored by the adsorption of water molecules from the humidity of the air humidity.¹⁷⁾ The weight losses of about 1–3.5 % and 4–5% in the respective temperature

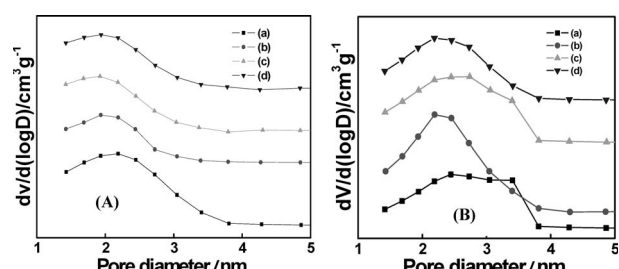


Fig. 2. Pore properties of (A) PWA/PMA– $\text{ZrO}_2\text{-P}_2\text{O}_5\text{-SiO}_2$ and (B) PWA/PMA– $\text{TiO}_2\text{-P}_2\text{O}_5\text{-SiO}_2$ glass composite membranes: (a) 1/1–2–5–91 (mol %), (b) 1/1–3–5–90 (mol %), (c) 1/1–4–5–89 (mol %) and (d) 1/1–5–5–88 (mol %) determined with the Brunauer–Emmett–Teller (BET) method.

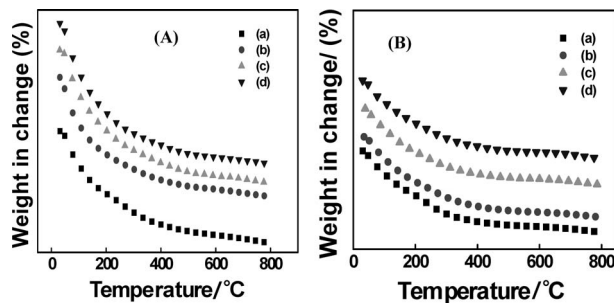


Fig. 3. TGA plots of (A) PWA/PMA-ZrO₂-P₂O₅-SiO₂ and (B) PWA/PMA-TiO₂-P₂O₅-SiO₂ glass composite membranes: (a) 1/1-2-5-91 (mol %), (b) 1/1-3-5-90 (mol %), (c) 1/1-4-5-89 (mol %) and (d) 1/1-5-5-88 (mol %).

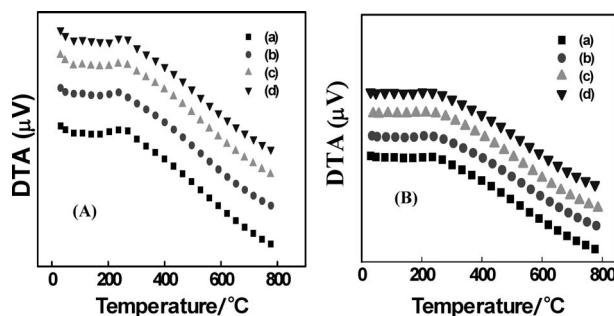


Fig. 4. DTA plots of (A) PWA/PMA-ZrO₂-P₂O₅-SiO₂ and (B) PWA/PMA-TiO₂-P₂O₅-SiO₂ glass composite membranes: (a) 1/1-2-5-91 (mol %), (b) 1/1-3-5-90 (mol %), (c) 1/1-4-5-89 (mol %) and (d) 1/1-5-5-88 (mol %).

ranges 200–450°C and 200–400°C, resulted from the desorption of chemisorbed water and hydroxyl groups via a strong hydrogen bonding in the structure. The weight loss in the final stage was ascribed to the removal of the adsorbed water and hydroxyl groups via strong hydrogen bonding to the oxygen atom of POH in the network structure of the glass membrane.

As demonstrated by Figs. 4(a) and (b), no endothermic peaks were observed in the DTA curves of any of the samples, indicating that no phase change took place. This indicates that the glass composite membranes consisted of a non-crystalline phase formation obtained by the sol-gel preparation. A rather broad exothermic peaks could be seen between 200 to 400°C for the associated weight loss (Fig. 4(a)) and slightly exothermic peaks appeared around 220°C (Fig. 4(b)). A broad exothermic peak was seen at approximately 250°C (Fig. 4(a)), the intensity of which was minimized in the PWA/PMA-TiO₂-P₂O₅-SiO₂ glass composite membrane (Fig. 4(b)). This result indicated that the addition of ZrO₂ and TiO₂ was effective for improving the thermal stability of the electrolyte. The results confirmed that the glass composite membranes were stable up to approximately 450°C. The tendency was similar for all samples, and this weight loss was assigned to the final thermal decomposition of the polymeric network as well as to the structural collapse of PWA/PMA with the loss of phosphorous. These changes can be associated to the glass transition, thus indicating that the amorphous materials were glassy systems.⁹⁻¹¹⁾ This has previously been confirmed for heteropolyacids incorporated with inorganic glass materials.

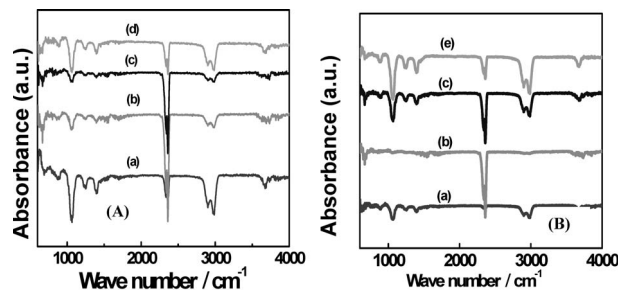


Fig. 5. FTIR spectra of (A) PWA/PMA-ZrO₂-P₂O₅-SiO₂ and (B) PWA/PMA-TiO₂-P₂O₅-SiO₂ glass composite membranes: (a) 1/1-2-5-91 (mol %), (b) 1/1-3-5-90 (mol %), (c) 1/1-4-5-89 (mol %) and (d) 1/1-5-5-88 (mol %).

3.3 FTIR study

Figures 5(a) and (b) show the structural information for the PWA/PMA-ZrO₂-P₂O₅-SiO₂ and PWA/PMA-TiO₂-P₂O₅-SiO₂ glass composite membranes. The inorganic Ti and Zr components, a broad and strong absorption band emerged in the range of 3400–3500 cm⁻¹, corresponding to unreacted Si-OH, Ti-OH and Zr-OH residues in the composites due to the low curing temperature. The band at 800 cm⁻¹ was believed to result mainly from the bending vibrations of Zr-O,¹⁸⁾ whereas the broad absorption band at 600 cm⁻¹ attributed to the Ti-O.¹⁹⁾ Peaks near 1200 and 1050 cm⁻¹ were respectively assigned to the asymmetric and symmetric stretching vibrations of PO₄ tetrahedra with two non-bridging and two bridging oxygen atoms attached to the phosphorous atom.²⁰⁾ The presence of a band at 950 cm⁻¹ suggested that the Zr⁴⁺ ions were preferentially bonded with the hydrolyzed SiOH groups, forming the Zr-O-Si bonds (Fig. 5(a)). This experimental result indicated that the amount of water bound to hydroxyl groups on the pore surfaces could be determined by a heat treatment at 600°C. The intensity of the absorption was representative of the Si-O-Si stretching modes at around 800–1300 cm⁻¹ and the intensity varied with the P₂O₅ content in the sample. The 1530, 1650, and 2350 cm⁻¹ bands were assigned to the hydroxyl related vibrational modes.²¹⁾ According to the data, absorption bands were seen with the titania-silica mixed oxides, suggesting that the absorption may be connected to the presence of Ti-O-Si bonds (Fig. 5(b)). The band at 2346 cm⁻¹ represented trapped CO₂ gas inside the remaining closed porosity. The main characteristics of a glass consist in the presence of Si-O-Si and PW-O-Si bonds, which can be identified by FTIR analysis. The PWA/PMA clusters were probably stabilized in the membrane through coulombic interaction and hydrogen bridges with the inorganic component, mainly the Si-OH groups.²²⁾ The stability of the heteropolyacids supported on titania increased due to these anionic support interactions as the HPAs could be linked to the titania surface by the strongest acidic protons. This resulted in Ti-OH₂⁺ groups that were able to strongly attract the HPAs through electrostatic interactions.²³⁾ The bands in the 1000–700 cm⁻¹ region were characteristic of the Keggin unit.²⁴⁾ From these observations, it could be concluded that HPA maintained its unique structure of heteropoly anion structure even after doping with the inorganic glass structure.

4. Summary

The present work has evaluated thermal, FTIR and textural properties of glass ceramic composite membranes of varying compositions synthesized via a sol-gel process. The porous glass

composite membranes displayed good thermal stabilities up to 450°C. The heteropolyacids were attracted to the membranes through coulombic interactions and hydrogen bridges with the inorganic component, mainly the Si-OH groups. The proton conductivity of these glass composite membranes will be determined by the impedance spectroscopy in future investigations. Their evaluation in fuel cell tests will also be necessary.

Acknowledgements The Japan Society for the Promotion of Science (JSPS) is gratefully acknowledged for their financial support.

References

- 1) A. M. Herring, *Polym. Rev.*, **46**, 245–296 (2006).
- 2) M. I. Ahmad, S. M. J. Zaidi and S. U. Rahman, *Desalination*, **193**, 387–397 (2006).
- 3) N. W. DeLuca and Y. A. Elabd, *J. Polym. Sci. B. Polym. Phys.*, **44**, 2201–2225 (2006).
- 4) A. Ainla and D. Brandell, *Solid State Ionics*, **178**, 581–585 (2007).
- 5) X. Cui, S. Zhong and H. Wang, *J. Power Sources*, **173**, 28–35 (2007).
- 6) M. Nogami, Y. Goto, Y. Tsurita and T. Kasuga, *J. Am. Ceram. Soc.*, **84**, 2553–2556 (2001).
- 7) M. Nogami, M. Suwa and T. Kasuga, *Solid State Ionics*, **166**, 39–43 (2004).
- 8) T. Uma and M. Nogami, *J. Non-Cryst. Solids*, **351**, 3325–3333 (2005).
- 9) T. Uma and M. Nogami, *J. Ceram. Soc. Japan*, **114**, 748–753 (2006).
- 10) T. Uma and M. Nogami, *J. Membr. Sci.*, **280**, 744–751 (2006).
- 11) T. Uma and M. Nogami, *Chem. Mater.*, **19**, 3604–3610 (2007).
- 12) C. J. Pierce, *J. Phys. Chem.*, **57**, 149–152 (1953).
- 13) K. Kaneko, *J. Membr. Sci.*, **96**, 59–89 (1994).
- 14) G. S. Armatas, C. E. Salmas, M. Louloudi, G. P. Androuloupolis and P. J. Pomonis, *Langmuir*, **19**, 3128–3136 (2003).
- 15) M. Nogami, Y. Goto and T. Kasuga, *J. Am. Ceram. Soc.*, **86**, 1504–1507 (2003).
- 16) C. Wang and M. Nogami, *Mater. Lett.*, **42**, 225–228 (2000).
- 17) M. Nogami and Y. Abe, *Phys. Rev. B*, **55**, 12108–12112 (1997).
- 18) T. Lopez, F. Tzompantzi, J. Hernandez-Vectura, X. Boxhimi, G. Pecchi, R. Retes and R. Gomez, *J. Sol-Gel. Sci. Tech.*, **24**, 207–219 (2002).
- 19) A. Pirson, A. Mohsine, R. Marchor, B. Michaux, O. W. Cantfort and J. R. Pirard, *J. Sol-Gel. Sci. Tech.*, **4**, 179–185 (1995).
- 20) K. Meyer, *J. Non. Cryst. Solids*, **209**, 227–239 (1997).
- 21) J. T. Braunholtz, G. E. Hall, F. G. Mann and N. Sheppard, *J. Chem. Soc.*, **29**, 868–872 (1959).
- 22) U. Lavrencic Stanger, N. Groselj, B. Orel, A. Schmitz and Ph. Columban, *Solid State Ionics*, **145**, 109–118 (2001).
- 23) S. Damyanova and J. L. G. Fierro, *Chem. Mater.*, **10**, 871–879 (1998).
- 24) C. Rocchiccioli-Deltcheff, R. Thouvenot and R. Franck, *Spectrochim. Acta.*, **A32**, 587–597 (1976).